

# Is the Collagen Primed for Mineralization in Specific Regions of the Turkey Tendon? An Investigation of the Protein–Mineral Interface Using Raman Spectroscopy

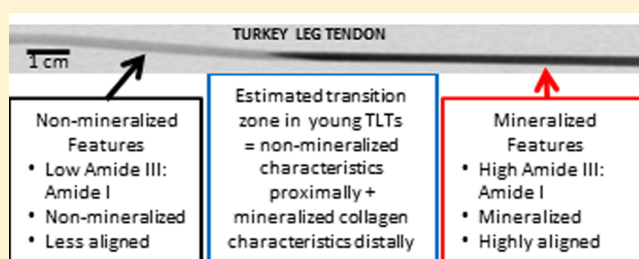
Jemma G. Kerns,<sup>\*,†,§</sup> Kevin Buckley,<sup>†,‡</sup> John Churchwell,<sup>†</sup> Anthony W. Parker,<sup>†,‡</sup> Pavel Matousek,<sup>†,‡</sup> and Allen E. Goodship<sup>†</sup>

<sup>†</sup>Institute of Orthopaedics and Musculoskeletal Science, University College London, Royal National Orthopaedic Hospital, Stanmore, Middlesex HA7 4LP, U.K.

<sup>‡</sup>Central Laser Facility, Research Complex at Harwell, STFC Rutherford Appleton Laboratory, Harwell Oxford, Oxfordshire OX11 0QX, U.K.

<sup>§</sup>Lancaster Medical School, Faculty of Health and Medicine, Lancaster University, Lancaster, Lancashire LA1 4YW, U.K.

**ABSTRACT:** The tendons in the turkey leg have specific well-defined areas which become mineralized as the animal ages and they are a thoroughly characterized model system for studying the mineralization process of bone. In this study, nondestructive Raman spectroscopic analysis was used to explore the hypothesis that regions of the turkey tendon that are associated with mineralization exhibit distinct and observable chemical modifications of the collagen *prior* to the onset of mineralization. The Raman spectroscopy features associated with mineralization were identified by probing (on the micrometer scale) the transition zone between mineralized and nonmineralized regions of turkey leg tendons. These features were then measured in whole tendons and identified in regions of tendon which are destined to become rapidly mineralized around 14 weeks of age. The data show there is a site-specific difference in collagen prior to the deposition of mineral, specifically the amide III band at  $1270\text{ cm}^{-1}$  increases as the collagen becomes more ordered (increased amide III:amide I ratio) in regions that become mineralized compared to collagen destined to remain nonmineralized. If this mechanism were present in materials of different mineral fraction (and thus material properties), it could provide a target for controlling mineralization in metabolic bone disease.



A number of bird species have tendons that ossify in specific regions to maximize the stiffness of the organ and thus improve its energy efficiency.<sup>1,2</sup> An example is the extensor tendon of the turkey leg which begins to mineralize proximal and distal to the tarsometatarsal joints when the bird is 10–14 weeks old.<sup>3,4</sup> This mineralization pattern creates two zones of “transition” (1–2 mm wide) between mineralized and nonmineralized tendon; one is one-third of the length of the organ from the proximal end, and the second is one-third of the length of the organ from the distal end (Figure 1).

The turkey leg tendon (TLT) is a well-characterized system and has been used to investigate the initiation and progression of mineralization. Electron microscopy of turkey tendons has been used to show initialization of mineralization in the gap regions between the ends of the collagen molecules and X-ray scattering has elucidated the nature of the lateral packing of the collagen molecules. The collagen fibrils become straighter and more tightly packed, with mineral deposited from the center of the tendon toward the proximal end.<sup>5</sup>

Biochemical analyses of the collagen from turkey tendons have shown that different post-translational modifications occur in regions of the TLT associated with future mineralization

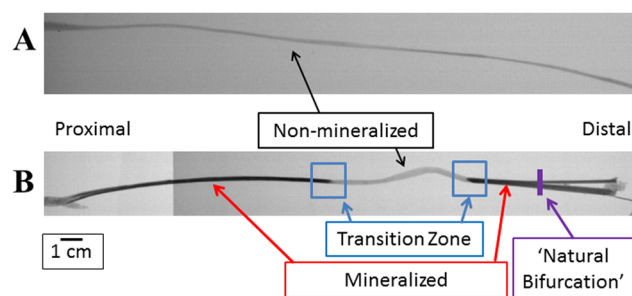


**Figure 1.** (A) Reverse gray scale radiograph of a (A) young, 11 week old turkey and (B) a tendon from an older, 18 week old turkey.

status, that collagen cross-linking in the mineralizing and nonmineralizing regions differ, and that the differences are present in young animals prior to mineralization (the transition zones were not analyzed in that study).<sup>6</sup> Lysyl hydroxylation

**Received:** January 30, 2015

**Accepted:** December 8, 2015

**Published:** January 13, 2016

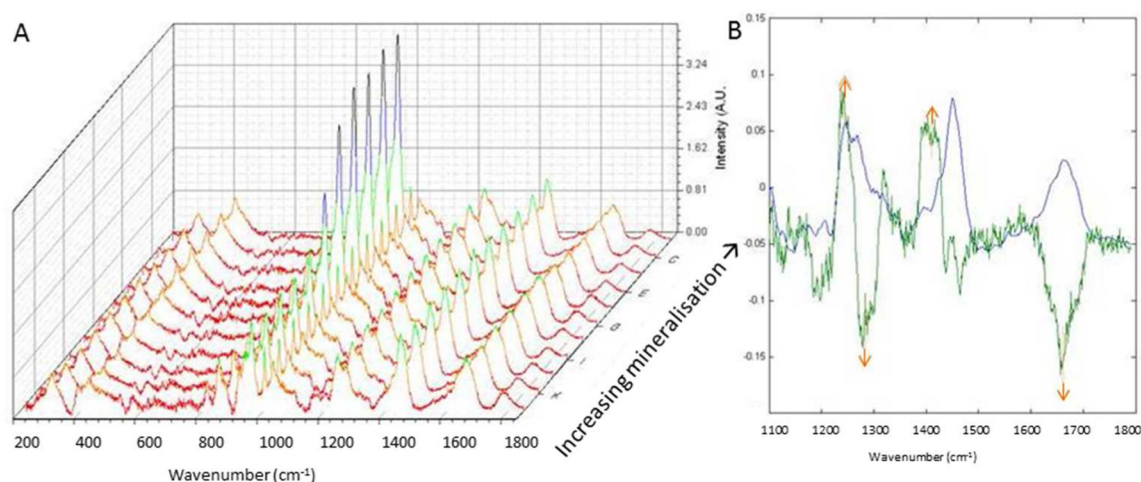


**Figure 2.** (A) Raman line map across the mineralization transition zone; (B) the phosphate bands increase as expected but the profiles of the protein bands also show prominent changes.

increases with age in nonmineralized and nonmineralizing regions of the TLTs, but it decreases in (future) mineralized regions. Furthermore, low levels of hydroxylysylpyridinoline and lysylpyridinoline are associated with a mineralized collagen matrix. It has been concluded that the areas of the TLT are predetermined to become mineralized by the change in cross-links and matrix metalloproteinase activities prior to mineralization.<sup>7</sup>

Vibrational spectroscopic techniques are useful for analyzing TLTs because they facilitate the assessment of both the organic and inorganic phases of the tissue nondestructively. Fourier transform infrared microspectroscopy (FTIRM) has been used to study the alignment of both the mineral and protein components of tendon tissue and the crystallinity of the hydroxyapatite across the mineralization transition zone.<sup>8</sup> Other infrared (IR) studies of mineralization in related connective tissues have also been reported; these include *in vitro* bone nodules,<sup>9</sup> microdamaged sections of bone,<sup>10</sup> cartilage,<sup>11</sup> and dental lesions.<sup>12</sup> FTIR studies of the turkey leg tendon itself have shown that the mineralization commenced in the middle of the tendon and progressed proximally, with the mineral subsequently maturing; that is, the more distal part of the tendon region is initially more mature than the proximal end (until mineralization is complete).<sup>13</sup>

Raman spectroscopy, like IR absorption, is a vibrational spectroscopy technique that is sensitive to both the organic and inorganic phases of mineralized tissue; it is complementary to FTIRM (chemically) but has an advantage in that it does not suffer from interference by the presence of water (and thus suitable for fresh whole organ analysis). Raman spectroscopy has previously been used to assess bone strength<sup>14</sup> and the profile of the amide I band (mainly carbonyl mode but with contributions from CN) has previously proven to be sensitive to mineralization status.<sup>15,16</sup>

In the present study, Raman spectroscopy is used to probe the nonmineralized, transitional, and mineralized regions of TLTs. Our study was as follows: (1) Probe the transition zone of mineralized turkey tendons to identify the Raman spectral markers that are associated with mineralization (i.e., mineralization causes the “collagen fibrils become straighter and more tightly packed”) and (2) identify these spectral features in older turkey tendons in mineralized and unmineralized regions.

We hypothesize that in the tendons of young turkeys the collagen develops, in a site-specific manner, in preparation for the deposition of mineral and that these site-specific differences can be investigated with Raman spectroscopy. To test this hypothesis, we probe younger (age 11 weeks) turkey tendons, along their lengths, to identify the relevant spectral features associated with mineralization.

## ■ MATERIALS AND METHODS

**Materials.** Twelve slaughtered turkeys were acquired from a local farm (Hertfordshire, UK). Six of the birds were 11 weeks of age (henceforth, “young” turkeys) and six were 18 weeks of age (“mature” turkeys). Both extensor tendons were removed from each animal by a veterinary surgeon and stored, fresh frozen, at  $-80\text{ }^{\circ}\text{C}$ .

**Data Collection.** Prior to Raman spectral interrogation, each tendon was thawed at ambient temperature and then radiographed (Faxitron 30 kV system).

The tendons were analyzed using a Renishaw *inVia* (Renishaw plc, Gloucestershire, UK) Raman microscope ( $\times 50$  objective) equipped with an 830 nm laser (laser power at the sample was  $\sim 10$  mW). Each tendon was analyzed in the same orientation. A minimum of 10 spectra (3 s accumulation) were acquired from each “mature mineralized” region, each “mature nonmineralized” region, and each young (non-mineralized) tendon. Additionally, spectra were acquired from a tendon before they were frozen (i.e., fresh) and after they had been returned to room temperature (i.e., thawed).

To match the location of the “future-mineralization” zone, the length of all the older tendons were measured and the zone recorded as “X% along the length”. The “future-mineralization” zone was defined as ranging from 17% to 21% (starting from the natural bifurcation at the distal end, Figure 1).<sup>17</sup> The same method was then applied to the younger tendons; specifically, the distal zone was  $\sim 20$  mm from the natural bifurcation at the distal end, and spectra were acquired from this position proximally in steps of  $5000\text{ }\mu\text{m}$  for 4 cm (Figure 1). The total number of spectra collected from each distal transition zone was 10, totaling 120 spectra.

**Data Analysis.** All spectra were baseline-corrected using a third-order polynomial (in house code, MATLAB, The Mathworks, Inc., Natick, MA, USA) and normalized to the amide III peak ( $1240\text{ cm}^{-1}$ ). For the mineralized regions the

mineralization ratio was calculated by dividing the intensity of the phosphate  $\nu_1$  band ( $\sim 960\text{ cm}^{-1}$ ) by the intensity of the hydroxyproline collagen band ( $870\text{ cm}^{-1}$ ). Other collagen analysis was performed using the amide III:amide I ratio ( $\sim 1250\text{:}\sim 1665\text{ cm}^{-1}$ ) and the proline:hydroxyproline ratio.

Principal component analysis (PCA; MATLAB, The MathWorks, Inc.) of the spectra was performed with the spectra classed according to the distance from the distal end of the tendon.<sup>18,19</sup> Scores and cluster vector plots were produced to visualize the spread of the data and the wavenumber variance, respectively. A cluster vector is a combination of all of the principal components directed through the mean of each class, enabling any distinction between them to be visualized.

## RESULTS

**Transition Zone.** The Raman spectral measurements across the mineralization transition zone (Figure 1) show that increasing mineralization (increasing phosphate band height) correlates ( $r^2 = 0.72$ ) with the amide III:amide I ratio ( $\sim 1250\text{:}\sim 1665\text{ cm}^{-1}$ ) increasing and the amide III band changing shape (orange arrows in Figure 2B); these spectral characteristics indicate that the mineralized tendon collagen is ordered to a greater degree (more aligned) than the less mineralized tendon and that the ratio of random-coil protein to  $\alpha$ -helical protein (amide III band  $1268\text{:}1244\text{ cm}^{-1}$ ) is greater.<sup>20</sup>

**Older Turkeys.** Radiographs confirm that the distal and proximal ends of all the tendons from the older turkeys are mineralized (Figure 1B). Spectra that were retrieved from the mineralized and nonmineralized regions of the older TLTs displayed obvious differences, specifically (and as expected), the former contained phosphate and carbonate peaks, the latter did not (Figure 3).

**Younger Turkeys.** Radiographs indicate that the tendons from the young turkeys are not mineralized (Figure 1A). Raman spectra confirmed that there was no mineral (lack of phosphate or carbonate peaks) in any of the young TLTs. Spectra from the future-mineralized and future nonmineralized

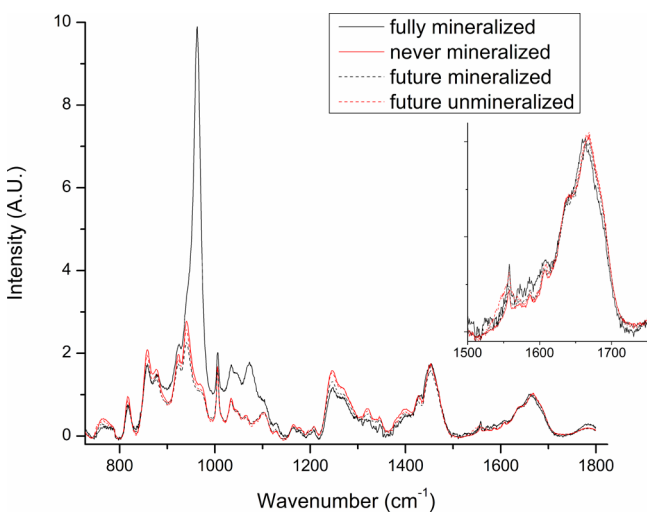


**Figure 3.** Protein bands in the mineralized regions (18 week old turkeys) are similar to those in regions that would have become mineralized (if the 11 week old turkey had matured). The nonmineralized regions (18 week old) have more similar spectra to the regions that would never have become mineralized (i.e., the amide III:amide I ratio is less, see inset).

regions of the tendons were very similar with no differences discernible by eye.

PCA and resultant two-dimensional (Figure 4B; the y-axis is for visualization purposes only) of the Raman spectra from the

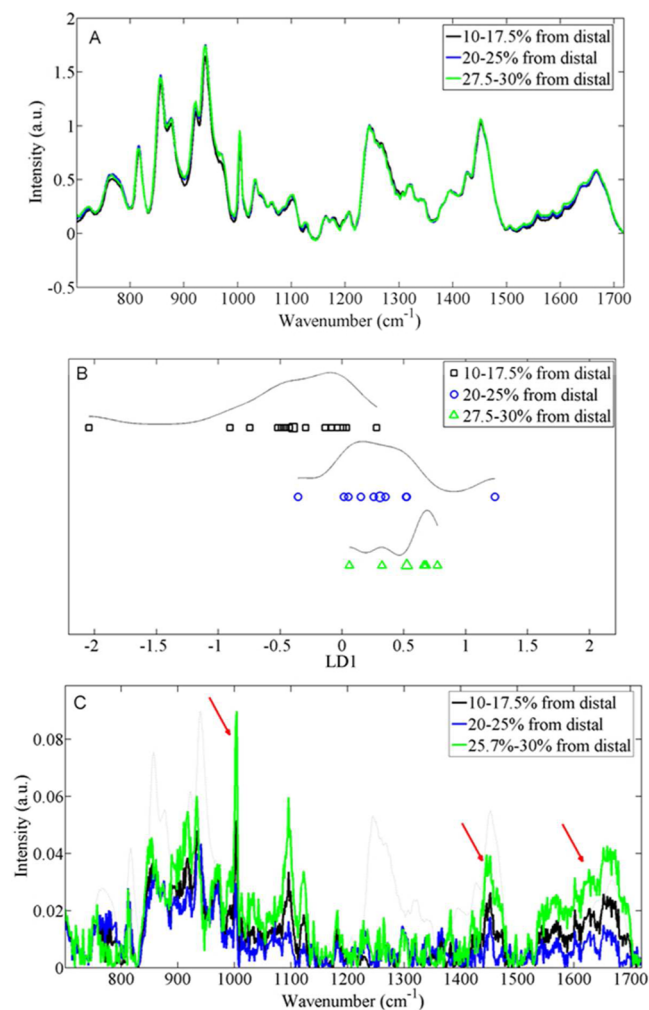


**Figure 4.** Raman spectra from the young turkey tendons, grouped based on distance from the distal end of the tendon. (A) Average spectrum from each region; (B) PCA scores plot of the three regions (black lines signify the spread); (C) corresponding cluster vector plot from (B), with arrows indicating the main changes along the tendon from distal to proximal.

young turkey tendons reveals that there is a transition along the axis of maximal variance (PC1), separating the spectra acquired from the distal side of the transition zone from those that were acquired from the proximal side of the transition zone. Furthermore, this spread reveals that there is more variance between the spectra acquired from the distal tendon compared to the spectra acquired more proximally. This spread of data can be explained by interpreting Figure 4C (cluster vector plots of Figure 4B): shows variation, mainly an increase in intensity across the amide I ( $1665\text{ cm}^{-1}$ ),  $\text{CH}_2$  ( $1450\text{ cm}^{-1}$ ), and phenylalanine ( $1000\text{ cm}^{-1}$ ) bands as the distance from the distal region is increased, that is moving toward the proximal region. The  $1650\text{ cm}^{-1}$  band (amide I) is less prominent, in relation to amide III, in the more distally acquired spectra, interpreted as being due to an alignment change in the collagen fibrils (the C–N bonds of the proline and hydroxyproline

become perpendicular to the collagen backbone). These features were also evident in the spectra acquired from the mineralized region of the mature tendon (Figure 3).

**Comparing Older and Younger Turkeys.** The spectra from the “future mineralized” and the “future nonmineralized” regions of young turkeys share similarities with the tendons from the older turkeys (Figure 4A); the distal (to-be-mineralized) section has an increased amide III:amide I ratio and a higher  $\text{CH}_2$  ( $1450\text{ cm}^{-1}$ ) band compared to spectra acquired more proximally (future nonmineralized region).

A direct comparison (Figure 3) of the spectral data from both sets of TLTs illustrates the main findings: the collagen spectra from the mineralized and “future-mineralized” regions of the tendons are similar, specifically across the amide III band where there is an increased  $1270:1240\text{ cm}^{-1}$  ratio compared to the nonmineralized tendons. There is a direct correlation between this ratio and the height of the phosphate band in the mineralized tendon. This ratio is increasing in the future-mineralized TLTs and provides evidence that the collagen changes occur prior to mineralization. Fundamentally, these data show that the collagen becomes more orientated and aligned. The collagen in the nonmineralized TLTs is comparable to the future nonmineralized regions of the young turkey tendons. The similarities and differences measurable prior to mineralization confirm that regions are predetermined and that an appropriate extracellular matrix (protein phase) structure is already in place.

Under the same conditions spectra were examined for freeze/thawing induced changes from nonmineralized fresh tendon before and after freezing, and were compared to the differences in collagen due to mineralization. Specifically, the amide III:amide I ratio of these frozen and thawed TLTs has a range of 0.074; comparatively, the difference in amide III:amide I of the nonmineralized TLTs has a range of 0.36.

## DISCUSSION

Distinct Raman spectroscopic differences were found between the mineralized and nonmineralized TLTs with the multivariate analysis revealing a gradual change in the protein profile across the future-mineralized regions. Along the length of the mature tendons the intensities of the mineral spectral peaks, particularly the phosphate mineral band (strong Raman scatterer), were correlated with position (% along the length) from the natural bifurcation at the distal end (Figure 1B). It has previously been shown<sup>17</sup> (using ashing methods) that mineral components are not present in turkey leg tendons at week 11 and it is generally agreed that mineralization does not commence until the bird is 12 weeks old, our data are in agreement with this consensus.

Previously published evidence also suggested that collagen becomes more aligned as the mineral fraction increases, our Raman data showed that as the phosphate Raman peak increased across the mineralisation zone the collagen band profile showed changes that are indicative of increased collagen alignment (i.e., increased amide III to amide I ratio).<sup>5</sup>

Mineralised collagen matrices have higher levels of lysylpyridinoline mature cross-links compared to nonmineralized matrices which have higher levels of hydroxylslypyridinoline.<sup>7</sup> The only chemical difference is the former has an OH bond, whereas the latter has a  $\text{CH}_2$  bond in the same position on the pyridinoline molecule. We also note the height of the  $\text{CH}_2$  band, as apparent in the Raman spectra at  $1450\text{ cm}^{-1}$ ,

drops in intensity relative to level of mineralization of the TLTs.

Changes in collagen structure are found across other mineralization interfaces, including tendon to bone of well-aligned type I collagen fibers, progressing through regions of type II and III collagen, to mineralized fibrocartilage, to mineralized bone, with continuous changes in structure across this fibrocartilaginous zone, to transfer load.<sup>21</sup> Furthermore, there is evidence to suggest that the collagen fibril alignment from tendon to bone where the axial contraction and lateral expansion of mineralized fibrils serve as the mechanism for the resultant strength of the attachment.<sup>22</sup> It has also been shown that the attachment of ligament to bone is based on a change in the collagenous alignment and structure utilizing calcified and uncalcified fibrocartilage.<sup>23,24</sup> The process of mineralization involves alkaline phosphatase, present in the extracellular matrix, providing the phosphate ions locally, and a prerequisite for tendon and ligament repair, naturally and in vitro, has been a collagen matrix.<sup>25,26</sup>

We should consider whether the freezing of the tendons during storage has any impact on our results as there is evidence that the freezing process induces changes in collagen; this would of course not affect the levels of mineralization. Our results comparing amide III:amide I before and after freezing, although a change was found, this was a magnitude smaller than differences found due to mineralization. We do not believe freezing has influenced our findings because all the tendons were treated in the same way (i.e., it was not the case that, for instance, the young tendons were frozen and the mature tendons were not).

As established, the spectra from the mineralized TLTs have a strong phosphate peak and an increased amide III:amide I ratio; in comparison, the future mineralized collagen matrix also exhibited changes in the amide III:amide I ratio. More specifically, there was an amide III shape change where the band at  $1270\text{ cm}^{-1}$  was increasing (in the regions where the collagen becomes more ordered).<sup>5</sup> This difference is apparent between the nonmineralized and future-mineralized one; that is, it is not present in the former. The lower degree of intracategory variance in the distally acquired spectra from the mineralization transition zone suggests that the collagen is different than that in the proximal region and is more aligned, perhaps supporting the theory that the matrix is turning over, forming an altered, more aligned, extracellular matrix to support the mineralization process. The use of PCA allowed us to objectively map the changes along the length of the tendons while comparing and contrasting young and mature tendons. The same chemical changes were found across tendons from turkeys in both ages, supporting the hypothesis.

## CONCLUSION

Raman spectroscopy has been used to study regions of TLTs that have different mineralization statuses, the technique allowing probing of the collagen and mineral simultaneously (at a spatial resolution of a few micrometers). The main finding is that there is a shift toward a more ordered (aligned) collagen matrix prior to the presence of mineral; this suggests that the areas of mineralization are predetermined. This work provides further detail on the mineralization process and suggests that Raman spectroscopy could facilitate the monitoring of a perturbed mineralization system.

## AUTHOR INFORMATION

### Corresponding Author

\*E-mail: j.kerns@lancaster.ac.uk (J.G.K).

### Author Contributions

All authors contributed to the writing of the manuscript. All authors have given approval to the final version of the manuscript.

### Notes

The authors declare no competing financial interest.

## ACKNOWLEDGMENTS

The authors would like to acknowledge Paul Christian (Royal Veterinary College) for sourcing the turkeys and Roberta Ferro de Godoy (UCL) for excising the tendons. The authors also thank the Engineering and Physical Sciences Research Council (EP/H002693/1), the Science and Technology Facilities Council, and University College London for their support.

## REFERENCES

- (1) Currey, J. D. *Bones: Structure and Mechanics*, 2nd ed.; Princeton University Press: Princeton, NJ, 2006.
- (2) Silver, F. H.; Christiansen, D.; Snowhill, P. B.; Chen, Y.; Landis, W. J. *Biomacromolecules* **2000**, *1* (2), 180–5.
- (3) Landis, W. J.; Kraus, B. L. H.; Kirker-Head, C. A. *Connect. Tissue Res.* **2002**, *43* (4), 595–605.
- (4) Bigi, A.; Ripamonti, A.; Koch, M. H. J.; Roveri, N. *Int. J. Biol. Macromol.* **1988**, *10* (5), 282–286.
- (5) Silver, F. H.; Freeman, J. W.; Seehra, G. P. *J. Biomech.* **2003**, *36* (10), 1529–53.
- (6) Knott, L.; Tarlton, J. F.; Bailey, A. J. *Biochem. J.* **1997**, *322*, 535–542.
- (7) Knott, L.; Bailey, A. J. *Bone*. **1998**, *22* (3), 181–7.
- (8) Gadaleta, S. J.; Camacho, N. P.; Mendelsohn, R.; Boskey, A. L. *Calcif. Tissue Int.* **1996**, *58* (1), 17–23.
- (9) Ghita, A.; Pascut, F. C.; Sottile, V.; Notingher, I. *Analyst* **2014**, *139* (1), 55–58.
- (10) Timlin, J. A.; Carden, A.; Morris, M. D.; Rajachar, R. M.; Kohn, D. H. Raman spectroscopic imaging markers for fatigue-related microdamage in bovine bone. *Anal. Chem.* **2000**, *72* (10), 2229–2236; retrieved from <http://www.ncbi.nlm.nih.gov/pubmed/10845368> 10.1021/ac9913560
- (11) Nicholson, C. L.; Firth, E. C.; Waterland, M. R.; Jones, G.; Ganesh, S.; Stewart, R. B. *Anal. Chem.* **2012**, *84* (7), 3369–3375.
- (12) Yang, S.; Li, B.; Akkus, A.; Akkus, O.; Lang, L. *Analyst* **2014**, *139*, 3107–3114.
- (13) Schwartz, A. G.; Pasteris, J. D.; Genin, G. M.; Daulton, T. L.; Thomopoulos, S. *PLoS One* **2012**, *7* (11), e48630.
- (14) Morris, M. D.; Finney, W. F.; Rajachar, R. M.; Kohn, D. H. *Faraday Discuss.* **2004**, *126*, 159.
- (15) Buckley, K.; Matousek, P.; Parker, A. W.; Goodship, A. E. *J. Raman Spectrosc.* **2012**, *43* (9), 1237–1243.
- (16) Buckley, K.; Kerns, J. G.; Birch, H. L.; Gikas, P. D.; Parker, A. W.; Matousek, P.; Goodship, A. E. *J. Biomed. Opt.* **2014**, *19* (11), 111602.
- (17) Landis, W. J.; Librizzi, J. J.; Dunn, M. G.; Silver, F. H. *J. Bone Miner. Res.* **1995**, *10* (6), 859–67.
- (18) Trevisan, J.; Angelov, P. P.; Carmichael, P. L.; Scott, A. D.; Martin, F. L. *Analyst* **2012**, *137* (14), 3202–15.
- (19) Martin, F. L.; Kelly, J. G.; Llabjani, V.; et al. *Nat. Protoc.* **2010**, *5* (11), 1748–1760.
- (20) Chi, Z.; Chen, X. G.; Holtz, J. S. W.; Asher, S. A. *Biochemistry* **1998**, *37* (9), 2854–2864.
- (21) Thomopoulos, S.; Marquez, J. P.; Weinberger, B.; Birman, V.; Genin, G. M. *J. Biomech.* **2006**, *39* (10), 1842–1851.
- (22) Quan, B. D.; Sone, E. D. *Bone* **2015**, *77*, 42–49.

(23) Subit, D.; Masson, C.; Brunet, C.; Chabrand, P. *Journal of the Mechanical Behavior of Biomedical Materials* **2008**, *1* (4), 360–367.

(24) Lu, H. H.; Thomopoulos, S. *Annu. Rev. Biomed. Eng.* **2013**, *15*, 201–26.

(25) Berendsen, A. D.; Smit, T. H.; Hoeben, K. A.; Walboomers, X. F.; Bronckers, A. L. J. J.; Everts, V. *Biomaterials* **2007**, *28* (24), 3530–3536.

(26) Rodrigues, M. T.; Reis, R. L.; Gomes, M. E. *J. Tissue Eng. Regen. Med.* **2013**, *7*, 673–686.